

Loop Shaping of Hybrid Motion Control with Contact Transition

Michael Ruderman*

Abstract—A standard motion control with feedback of the output displacement cannot handle unforeseen contact with environment without penetrating into the soft, i.e. viscoelastic, materials or even damaging the fragile materials. Robotics and mechatronics with tactile and haptic capabilities, and in particular medical robotics for example, place special demands on the advanced motion control systems that should enable the safe and harmless contact transitions. This paper shows how the basic principles of loop shaping can be easily used to handle sufficiently stiff motion control in such a way that it is extended by sensor-free dynamic reconfiguration upon contact with the environment. A thereupon based hybrid control scheme is proposed. A remarkable feature of the developed approach is that no measurement of the contact force is required and the input signal and the measured output displacement are the only quantities used for design and operation. Experiments on 1-DOF actuator are shown, where the moving tool comes into contact with grapes that are soft and simultaneously penetrable.

I. INTRODUCTION

Motion control systems that can come into precisely defined or (more importantly) unpredictable contact with objects in the environment have always been the focus of active research, especially in the field of control and robotics, and have done so since the eighties of the last century. For instance, the dynamics stability issues during a contact with stiff environments were recognized and addressed (often in context of industrial robotics), see [1], when a manipulator in the force control mode comes in touch with a stiff and kinematically constrained environmental object. A milestone was the introduction of the concept of impedance control [2] and later of hybrid impedance control [3], which enabled a deep understanding of the most important (i.e., physically justifiable) interactions and constraints for the controlled impedance-admittance pair of a mechanical motion system in contact with its environment. Motion control of an unconstrained manipulation, on the one hand, and force control of a constrained interaction between the manipulator and its environment, on the other hand, became quickly to 'stumbling block', especially in view of controlling *contact transitions*, see e.g. discussion with experiments in [4]. For a former compact survey of the force control of manipulators we refer to e.g. to the work [5], while a more recent overview of the force control can be found in the robotic literature like e.g. Springer Handbook of Robotics [6].

The ideas of impedance and admittance control of robotic manipulators, [2], [3], found quickly a way and appreciation in motion control for drives and mechatronic systems [7]. A unified passivity-based control framework for position,

torque and impedance control, which uses the full state feedback and a dedicated energy shaping with variable gain strategy was also proposed in [8]. Another focus on decomposing (correspondingly switching) the control structure led to *hybrid position/force* controllers, the first one (most probably) proposed in [9]. A widely adopted strategy of hybrid force/motion control, which aims at controlling the motion along the unconstrained task directions and the force along the constrained task directions, is using a certain decomposition which allows simultaneous control of both the contact force and end-effector motion in two mutually independent subspaces, see [6] for details. Here, a selection strategy for the stiffness/compliance parameters and the desired and feeded back variables must be part of the overall control law and is known to be non-trivial and fundamental for the specification of the control task. Although impedance modulation and reconfiguration (correspondingly switching) are widely used in the hybrid position/force control in robotics, see e.g. [10], equally as in other motion control systems such as hydraulic actuators [11], the problems of transition and stability of the structural switching [12] remain among the most relevant. It should be emphasized that during a contact transition, both a hybrid position/force control and the process plant itself undergo a structural change. For sufficiently damped contact transitions and a relatively slow dynamics of an available internal state variable that experiences a threshold value upon contact, a switching strategy based on hysteresis relays can be applied, see e.g. [13]. For combining the robustness property of an impedance control in the stiff contacts with the accuracy of an admittance control in the soft contacts, various approaches were proposed in robotics. For instance, a predictive instantaneous model impedance control scheme was described in [14], and a continuous switching (with duty cycle as design parameter) between the controllers with impedance and admittance causality was provided (also with experiments) in [15].

An important causality constraint is that no one motion system can simultaneously impress a force on its environment and impose a displacement or velocity on it. Only one of both control variables, either interaction force or relative motion of the environmental object, can be determined along each degree of freedom [2]. This results from an instantaneous power flow between two or more physical systems. Recall that the power flow is definable as product of an *effort* and a *flow* variable, the force and velocity for mechanical systems, respectively. Given these basic principles, it seems obvious that different control concepts and an approach for combining them are required to control the unconstrained and constrained motion and the resulting contact force.

* University of Agder. Contact: michael.ruderman@uia.no
Author's accepted manuscript

A frequently appearing question is nevertheless how to handle those manipulator-environment configurations where the control design is a-priori constrained by some given structure and/or application specification and, most importantly, by the available sensors and their arrangement.

In this work, an intuitively understandable (for standard control design in frequency domain) approach of reshaping the otherwise stiffly designed feedback controllers is proposed. This way, a smooth and stable contact transition can be guaranteed without applying a more complex control structure. Most importantly, only the measured output displacement is used for feedback and the designed hybrid motion control does not require additional force sensors or observers of internal states. The rest of the paper is organized as follows. In section II, we discuss the types of impedance operators that represent an interaction with environment and relate them to the control loop properties required for a contact transition. Section III introduces the thereupon based hybrid motion control design. A detailed experimental case study with soft but penetrable grape objects coming into contact with the feedback controlled mechanical tool is provided in section IV. Brief conclusions are in section V.

II. IMPEDANCE AND SHAPING OF DISTURBANCE SENSITIVITY FUNCTION

For motion control at large, with one relative degree of freedom x specified in the generalized coordinates, one can define the *control stiffness*, cf. [7], [16], as

$$\kappa = \left. \frac{\partial f(\cdot)}{\partial x(t)} \right|_{t \rightarrow \infty}. \quad (1)$$

Here $f(\cdot)$ is the overall net force (in the generalized coordinates) imposed on the moving body of the motion control system under consideration. For a matched disturbance force $F(t)$ and a feedback control value $u(t)$, which inherently has dimension of force in the motion control, the total net force can be considered as a superposition $f = u + F$. Indeed, when a generic motion control system

$$\dot{y} = g(y, u, t) \quad (2)$$

with the sufficiently smooth flow map $g(\cdot)$ and the vector of states variables $y \in \mathbb{R}^n$ (often a vector of relative displacements and velocities) is in the steady-state, the control should balance the counteracting disturbance. Let us next fix some controlled operation point, in terms of (u_0, x_0) , and consider this way reduced (1) in the Laplace domain. Then, one can write

$$\tilde{\kappa}(s) = \frac{F(s)}{x(s)}, \quad (3)$$

provided that the Laplace transform of the control stiffness operator exists. Also we note that an equivalence between κ and $\tilde{\kappa}$ is valid only for low frequency range, cf. [3]. Recalling that for a linear environment, an *impedance* is defined as the ratio of the Laplace transforms of effort and flow [17], the mechanical impedance is (symbolically) written as

$$Z(s) = \frac{\text{force}(s)}{\text{velocity}(s)}, \quad (4)$$

that leads to a generic relationship

$$\tilde{\kappa}(s) = Z(s)s. \quad (5)$$

Since a dynamic interaction between two physical bodies implies that one must complement the other – i.e. along any degree for freedom if one is an impedance then the other must be admittance and vice versa [2] – the condition (5) becomes crucial. It reveals how the motion control system can be designed when an environment is classified by $Z(s)$.

Using the mechanical impedance definition (4), one can classify the following (typical) contact environments, which are associated with the corresponding impedance operators. The first one is the viscous dashpot, shown schematically in Fig. 1 (a). The constitutive equation of the Newtonian fluid

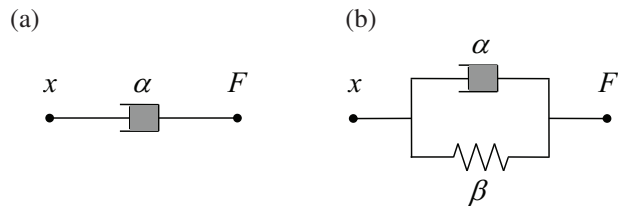


Fig. 1. Schematic representation of the contact environments: (a) viscous dashpot, (b) viscoelastic (Kelvin-Voigt type) contact.

in a dashpot, i.e. $F = \alpha \dot{x}$ where $\alpha > 0$ is viscosity, results in $Z_v(s) = \alpha$, meaning the contact environment is resistive, cf. [17]. If one expects the environment to be viscoelastic, i.e. to exhibit also a certain capacitive behavior, then one can assume a Kelvin-Voigt contact, that is schematically shown in Fig. 1 (b). This leads to the corresponding impedance operator $Z_{ve}(s) = \alpha + \beta/s$. Note that for modeling the environmental impedance, more complex structures than those shown in Fig. 1 can equally be assumed, and even variable and nonlinear structures might be considered. This would, however, go far beyond the scope of this work, and it turns out to be superfluous for a straightforward design of the linear and hybrid motion controllers.

Now, consider the loop transfer function

$$L(s) = C(s)G(s) \quad (6)$$

of the motion control system with the input-output plant $G(s) = x(s)(u(s) + F(s))^{-1}$ and feedback controller $C(s)$. The latter receives the control error $e(s) = r(s) - x(s)$ as input. Obviously, the control reference command $r(s)$ conforms to some application-related specifications before and after a possible contact with environment and without it. While the reference-to-output transfer function $H(s) = L(s)(1 + L(s))^{-1}$ can be determined by shaping $L(s)$, correspondingly by designing $C(s)$ to be possibly stiff, i.e. having possibly high bandwidth of $H(s)$ and possibly unity $|H(j\omega)|$ for all angular frequencies $\omega \in (0, +\infty)$, we focus on the disturbance response to $F(s)$ in the following. The disturbance-to-output transfer characteristics are given by

$$S(s) = \frac{x(s)}{F(s)} = \frac{G(s)}{1 + L(s)} \quad (7)$$

and often denoted as *disturbance sensitivity function*, cf. e.g. [18]. While an ideal position (or velocity) controller should not allow any steady-state or transient deviations for any force imposition on the mechanical system, i.e. the controller stiffness should be infinite, cf. [7], a hybrid motion controller with contact transition should allow $S(s)$ to match the $Z(s)$ properties of the contact with environment. Comparing (3), (5), and (7) one can recognize that

$$S(s) = \tilde{\kappa}^{-1}(s) = \frac{1}{Z(s)s}. \quad (8)$$

To further interpret the results obtained above, it is worth recalling a fundamental distinction between a mechanical admittance and impedance [2]. Multiple physical systems can be described in one form but not in the other. For instance, elastic contacts approximated by a non-monotonic constitutive equation can only be seen as impedance, i.e. $x \mapsto F$, but not as admittance. Indeed, prior to a mechanical contact is established, the map $F \mapsto x$ is not given. Similar issue appears in case of a tangential kinetic friction force, cf. [19]. Nevertheless, the admittance of the motion control, which is equivalent to disturbance sensitivity function (7), can certainly be used at the same moment as the mechanical contact with environment arises. This will be discussed and used further below in the derivation of hybrid motion control.

III. HYBRID MOTION CONTROL

First, we proceed with designing a (sufficiently) stiff feedback motion control denoted by C_s . Following the most simple loop shaping methodology and assuming the critically damped dominant pole pair of the closed-loop control system, the reference-to-output transfer function yields

$$H(s) = \frac{L(s)}{1 + L(s)} = \frac{\omega_0^2}{s^2 + 2\omega_0 s + \omega_0^2}. \quad (9)$$

The control specification is then given by only the natural frequency ω_0 (approximately equal to the bandwidth) of the closed-loop. Recall that higher ω_0 values imply higher stiffness of the controlled system. Using the given system transfer function $G(s)$ and applying the block diagram algebra, the resulting motion control $C_s(s) = L(s)G^{-1}(s)$ is

$$C_s(s) = \frac{\omega_0^2}{G(s)s(s + 2\omega_0)}. \quad (10)$$

Note that for the system plants $G(s)$ with a relative degree ≤ 2 , the control (10) yields a proper transfer function and, thus, can be directly implemented.

Now, for designing an impedance controller, assume a sensitivity function, cf. (8),

$$S_v(s) = \frac{1}{\alpha s}, \quad (11)$$

that corresponds to a viscous (dashpot-type) contact with environment, cf. section II. Using (7) and the block diagram algebra, the resulting impedance controller (denoted further as viscous) is determined by

$$C_v(s) = \frac{\alpha s G(s) - 1}{G(s)}. \quad (12)$$

Note that (12) reveals an improper transfer function so that an additional low-pass filter with a sufficiently high cut-off frequency needs to be applied in series with $C_v(s)$.

The magnitude response of $G(j\omega)$, $H(j\omega)$, $S_s(j\omega)$, and $S_v(j\omega)$ transfer functions are depicted in Fig. 2 for an exemplary assumed system plant with two negative real poles at $\{-1000, -10\}$, and the design parameters $\omega_0 = 100$ and $\alpha = 100$. Note that both disturbance sensitivity functions are determined according to (7) for each of the feedback controllers C_s and C_v . It is easy to interpret

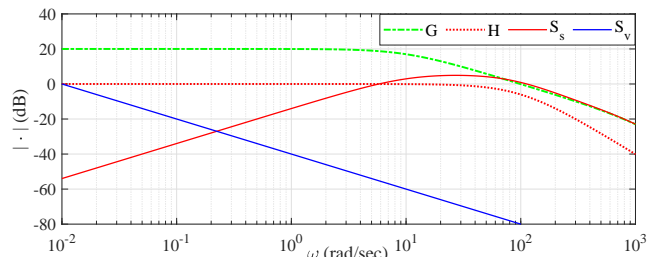


Fig. 2. Magnitude response of $G(j\omega)$, $H(j\omega)$, $S_s(j\omega)$, and $S_v(j\omega)$.

from the Bode plot of $S_s(j\omega)$ that a step-wise disturbance $F(s)$, which appears at the contact instant, will be largely suppressed by the stiff motion control. Following to that, the controlled mechanical motion system will continue to move and penetrate into the environmental object, or moves it away from itself if the latter is not fixed. Quite the opposite, the viscous impedance control will react to the step-wise contact force F by inducing a repulsive relative displacement in the opposite direction. Here it is worth noting that since it leads to release from the contact, the disturbance becomes zero and the relative motion will stop, cf. below with the experiments.

Recall that for achieving stable and smooth contact transitions, a general strategy of the motion control is to regulate the system displacement and/or velocity (as conventional manipulators do) and provide additionally a well-specified disturbance response for deviations from this motion. According to [2], such disturbance response has the form of an impedance, that may be then modulated and adapted depending on the control tasks and environment. Despite such straightforward impedance paradigm, that gives the name 'impedance control' [2], one task that is not always solvable remains the detection of contact, correspondingly recognition of the associated deviations from a well-specified (i.e. nominal) motion. Mostly, the contact forces are measured by a force sensor connected to the wrist of manipulator or integrated in the front-end tool. The use of internal (i.e. not only output displacement) measurements or even external sensors can be found both in the theoretical works, cf. e.g. [20] and experimental studies in robotics, e.g. [21], [10].

If the controlled output displacement is the only measurable state of a motion system (the case that we also consider in this work), the control reshaping can be triggered exclusively by an information content of the control signal. Assuming some nominal bound of the control signal U , that is mostly possible for the given nominal plant $G(s)$,

control $C_s(s)$, and reference $r(s)$, an overshoot $|u(t)| > U$ will indicate the appearance of a disturbance force F . Note that this strategy can be used in particular when the stiff motion controller C_s contains an integral control action. Indeed, during a compensated steady-state motion, an exceeded control force is proportional to an additional disturbing force. Since a dynamic transition from C_s to C_v should not provoke any undesired transients in direction of the contact with environment, it is worth examining the disturbance-to-control-value transfer characteristics which are given by $U(s) = u(s)/F(s) = C(s)G(s)(1 + C(s)G(s))^{-1}$. For both controllers (10) and (12), as designed exemplarily above, this is shown by the magnitude response in Fig. 3. One

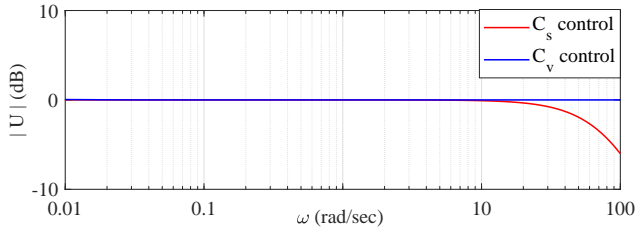


Fig. 3. Magnitude response of $U(j\omega)$ for C_s and C_v controllers.

can recognize that since r is set to zero for C_v , and the control magnitude response of both C_s and C_v have nearly the same value, an appearance of the step-wise disturbance $F(t_c)$ at $t = t_c$ will lead to a decrease of $|u(t_c)| = U$ by the magnitude equal to $|F|$ for $t > t_c$. Then, the force imposed on the environmental object under contact drops respectively.

IV. EXPERIMENTAL CASE STUDY

A. Motion system and contact scenarios

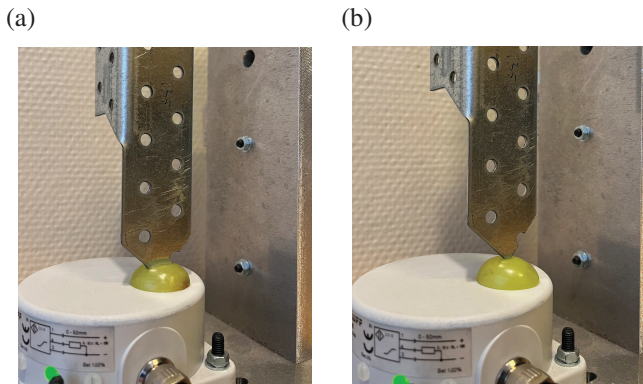


Fig. 4. Experimental setup of the controlled motion in contact with a soft environment – final steady phase after contact with a grape: (a) stiff motion control C_s , (b) hybrid motion control $C_s \rightarrow C_v$ with reshaped sensitivity.

In the following, we demonstrate an experimental case study of the proposed hybrid motion control with a smooth transition when the moving tool experiences unforeseen contact with environment. The latter is soft yet penetrable, emulating one of the most critical applications of the motion control – robotic assistance for medical diagnosis and surgery. For that purpose, a half of the grape is placed

in the way of the moving mechanical tool, see Fig. 4, which is controlled by using only the displacement feedback. The relative displacement of the tip of the tool is sensed remotely, i.e. contactless, cf. Fig. 4. Note that the way how the vertical displacement x is measured provides a relatively high level of the noise and, thus, represents rather a worst case scenario for the control application. The system input v (in volt) and output x (in meter) are the only quantities available for the control design and operation. The experimental motion system is actuated by a voice-coil-motor and has one translational degree of freedom. The rigid mechanical tool is moving in the vertical direction and has a relatively low displacement range about 0.015 m. The implemented feedback control is running on the dedicated real-time board with the set sampling rate of 10 kHz. For more technical details, including the physical system parameters, an interested reader is referred to [22].

The nominal system model is given by

$$x(s) = G(s)v(s) - D = \frac{K}{s(\tau s + 1)}v(s) - D, \quad (13)$$

where s is the Laplace variable, and K and τ are the known system gain and time-constant parameters, respectively. The constant term D constitutes the nominal disturbance due to the gravity force which is known. Therefore, the latter is pre-compensated, so that the system input signal results in

$$v(t) = D + u(t),$$

where the feedback controller output u is designed as described above in section III.

Due to a free integrator, cf. (13), the identification of the free system parameters was performed in a closed-loop configuration, see [23] for details. The least-squares determined parameter values are $K = 0.0408$ and $\tau = 0.00668$ sec, while the experimentally measured and identified magnitude response are shown over each other in the Bode diagram in Fig. 5. Note that an additional electrical time constant of

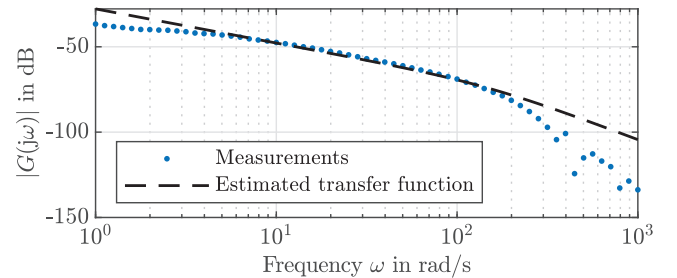


Fig. 5. Experimentally measured and least-squares identified magnitude response of the system input-output transfer function $G(j\omega)$.

the voice-coil-motor dynamics, which is about 0.0012 sec, is not explicitly taken into account, equally as not a minor time delay in the input-output loop of the system. Both are neglected in the nominal model (13), cf. [23]. At the same time, they constitute an additional robustness criterion for the motion control system under evaluation and, this way, contribute to a worst-case scenario under evaluation.

B. Evaluated motion control

For a sufficiently stiff motion control, i.e. the one without contact transition and featuring $|e(s)/F(s)|_{s \rightarrow 0} \rightarrow 0$, a standard PID (proportional-integral-derivative) controller

$$u_s(s) = C_s(s)e(s) = (k_p + k_i s^{-1} + k_d s) e(s), \quad (14)$$

is assumed. The controller transfer function is considered as 'stiff' and denoted by C_s . The applied robust design procedure, provided in [23], rests on an underlying PD control with a stable pole-zero cancellation (i.e. canceling the plant time constant τ) and an upper bound of the disturbance sensitivity function. The determined this way control parameters are $k_p = 429$, $k_i = 4348$, and $k_d = 2.67$.

Two reshaped 'soft' feedback controllers which allow for a stable and smooth contact transition are designed in accord with section II. The first one, denoted by $C_v(s)$, is enabling a purely viscous and well-damped repulsive behavior when contacting with environment, and it yields

$$u_v(s) = -\frac{0.0486 s^2 + 10.78 s}{(0.0272 s + 4.08)(\omega_c^{-1} s + 1)} x(s). \quad (15)$$

Another reshaped feedback controller, denoted by $C_{ve}(s)$, is more 'stiff' and enables for a viscoelastic behavior when contacting with environment, cf. section II. The resulting controller has the form

$$u_{ve}(s) = -\frac{0.0486 s^2 + 10.78 s}{(0.0272 s + 4.08)(\omega_c^{-1} s + 1)} x(s) + 429 e(s), \quad (16)$$

which is similar to (15) but differs from this by including also a proportional feedback of the control error, cf. with (14). The latter makes it possible to press on the environment with a force that is either proportional to the control error (in this case the reference value $r(t)$ is to be considered additionally), or with a constant force equal to U . For the

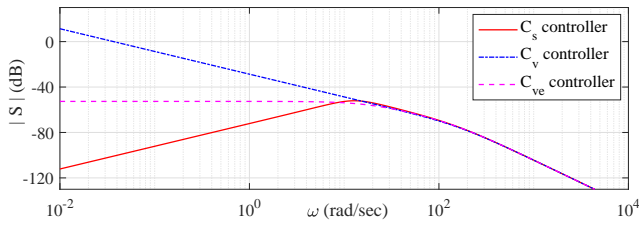


Fig. 6. Magnitude response of the disturbance sensitivity function for all three designed and evaluated feedback controllers $C_s(s)$, $C_v(s)$, $C_{ve}(s)$.

second case, which is used in the below experiments, the proportional control part in (16) is extended by saturation, i.e. $\text{sat}_U[k_p e(t)]$. Further we note that both fractions in (15) and (16) use a low-pass filter with a sufficiently high cut-off frequency ω_c ; otherwise both control transfer functions are improper and could not be implemented, cf. section III.

The resulted magnitude response of the closed-loop disturbance sensitivity functions $S(s)$ are compared for all three feedback controllers (here for $r = 0$) in Fig. 6.

The experimentally evaluated motion control scenario is shown in Fig. 7 (a). The reference trajectory $r(t)$ with one

positive and one negative slope, both implying the same reference velocity magnitude, is tracked by the designed stiff controller (14). On the way back, at time $t > 10$ sec, there is no environmental obstacles and, therefore, no contact with soft objects, cf. with Fig. 4 where a soft object was afterwards placed. Note that at the beginning and especially after the slope segments of trajectory, the control error $|e(t)|$ increases and takes certain time to settle, cf. Fig. 7 (a). This is due to nonlinear friction effects (see [19], [24] for details) which are not explicitly compensated and need to be mitigated by the proportional and integral feedback actions only. The output of the feedback controller $u(t)$ is depicted

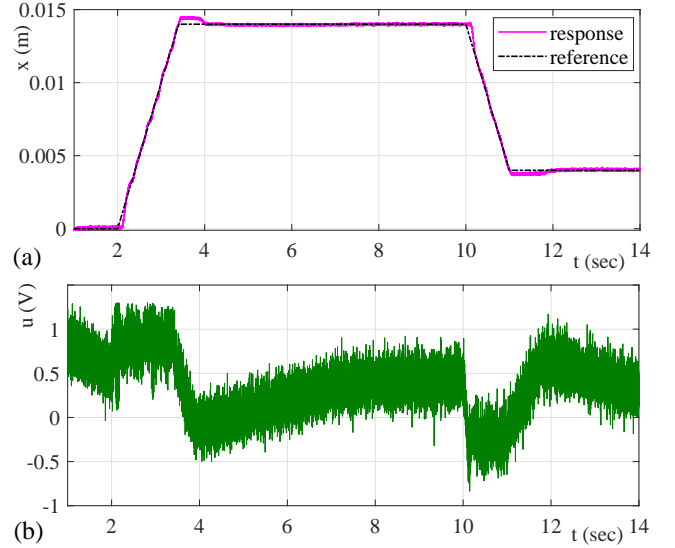


Fig. 7. Control response without contacting environment: (a) measured displacement $x(t)$ against reference $r(t)$, (b) control signal $u(t)$.

in Fig. 7 (b), indicating that it stays in a certain bound. The control reshaping threshold is set to $U = 1.3$. Recall that once $|u(t)| > U$, the feedback control changes from its stiff configuration, i.e. (14), to a compliant one, i.e. either (15) or (16) since both controllers C_v and C_{ve} were evaluated. Also recall that the reshaping threshold value corresponds to the disturbance force which increases once the stiff motion controller C_s is loading the contacting object, cf. section II.

Following to that, the experimental scenarios with a soft environmental object, which is a half of the grape placed before the way back i.e. at time $4 < t < 10$ sec, were evaluated. The final state is exemplified in Fig. 4. Three control configurations were evaluated. The first one is the stiff control (14) without hybrid reconfiguration to a compliant controller. The second is the stiff control (14) which is reconfigured to the viscous control (15) upon the reshaping threshold U . Finally the third is the stiff control (14) which is reconfigured to the viscoelastic control (16) upon the reshaping threshold U . Recall that the viscoelastic control (16) is additionally subject to the saturation at $|u(t)| = U$ since it contains also the feedback proportional to e . The measured displacement response $x(t)$ and the feedback control value $u(t)$ are shown in Fig. 8 (a) and (b), respectively. One can

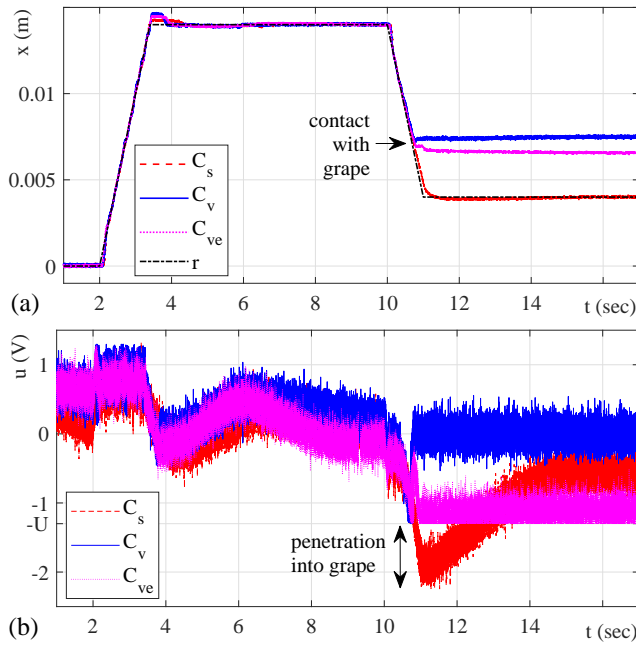


Fig. 8. Control response with contacting environment, comparing motion controller C_s with hybrid $C_s \rightarrow C_v$ and $C_s \rightarrow C_{ve}$ reshaping: (a) measured displacement $x(t)$ against reference $r(t)$, (b) control signal $u(t)$.

recognize that the stiff control C_s reaches the back reference position (for $t > 10$ sec), thus ploughing the mechanical tool into the soft environment, cf. Fig. 4 (a). Its control value falls below the set threshold and represents the corresponding force required to penetrate into the grape. Quite the opposite, the viscous control C_v , activated by exceeding the threshold value, provides a slightly repulsive response which can be associated with certain elasticity of the grape surface, cf. Fig. 4 (b). The controller C_v maintains the contact position while the control value has a zero mean and almost the same high frequency pattern as the C_s control has; this is due to the sensor noise and the corresponding output derivative. A slightly differing behavior can be seen in case of the viscoelastic controller C_{ve} . Due to a sufficiently large control error $e(t)$ for $t > 11$ sec and, at the same time, the used control saturation in C_{ve} , the motion system does not penetrate into the grape, but presses it further with the corresponding threshold magnitude.

The illustrative videos of two of the control experiments reported above, i.e. with the 'stiff' (PID) control (14) and the 'soft' viscous control (15), can be found online at <https://drive.google.com/file/d/1M9Y3YcCdRDVJ4cOXlq45WOhGyT5Jv4II> <https://drive.google.com/file/d/1JrF01yRCI6ZqB6PMSpZ19hkjczP8zLX> respectively.

V. CONCLUSIONS

In this communication, we provided an easily interpretable (in frequency domain) analysis and design for dynamically transforming stiff (admittance) motion control into soft (impedance) control upon contact with constrained and deformable environmental objects. Only the measured output

displacement is used. A hybrid control scheme was established, and insightful control experiments involving contact with soft but penetrable objects, e.g., grapes, were conducted.

REFERENCES

- [1] C. An and J. Hollerbach, "Dynamic stability issues in force control of manipulators," in *American Control Conference*, 1987, pp. 821–827.
- [2] N. Hogan, "Impedance control: An approach to manipulation: Part I – theory," *Transactions of the ASME*, vol. 107, no. 1, pp. 1–7, 1985.
- [3] R. Anderson and M. Spong, "Hybrid impedance control of robotic manipulators," *IEEE Journal on Robotics and Automation*, vol. 4, no. 5, pp. 549–556, 1988.
- [4] J. Hyde and M. Cutkosky, "Controlling contact transition," *IEEE Control Systems Magazine*, vol. 14, no. 1, pp. 25–30, 1994.
- [5] T. Yoshikawa, "Force control of robot manipulators," in *IEEE International Conference on Robotics and Automation*, 2000, pp. 220–226.
- [6] L. Villani and J. De Schutter, "Force control," in *Springer Handbook of Robotics*, pp. 195–220, 2016.
- [7] K. Ohnishi, N. Matsui, and Y. Hori, "Estimation, identification, and sensorless control in motion control system," *Proceedings of the IEEE*, vol. 82, no. 8, pp. 1253–1265, 1994.
- [8] A. Albu-Schäffer, C. Ott, and G. Hirzinger, "A unified passivity-based control framework for position, torque and impedance control of flexible joint robots," *The International Journal of Robotics Research*, vol. 26, no. 1, pp. 23–39, 2007.
- [9] M. Raibert and J. Craig, "Hybrid position/force control of manipulators," *ASME Journal of Dynamic Systems, Measurement, and Control*, vol. 103, no. 2, pp. 126–133, 1981.
- [10] F. Ficuciello, L. Villani, and B. Siciliano, "Variable impedance control of redundant manipulators for intuitive human–robot physical interaction," *IEEE Tran. on Robotics*, vol. 31, no. 4, pp. 850–863, 2015.
- [11] P. Pasolli and M. Ruderman, "Hybrid position/force control for hydraulic actuators," in *IEEE 28th Mediterranean Conference on Control and Automation (MED)*, 2020, pp. 73–78.
- [12] D. Liberzon and A. S. Morse, "Basic problems in stability and design of switched systems," *IEEE Control Systems Magazine*, vol. 19, pp. 59–70, 1999.
- [13] M. Ruderman, "On switching between motion and force control," in *IEEE 27th Mediterranean Conference on Control and Automation (MED)*, 2019, pp. 445–450.
- [14] T. Valency and M. Zacksenhouse, "Accuracy/robustness dilemma in impedance control," *ASME Journal of dynamic systems, measurement, and control*, vol. 125, no. 3, pp. 310–319, 2003.
- [15] C. Ott, R. Mukherjee, and Y. Nakamura, "A hybrid system framework for unified impedance and admittance control," *Journal of Intelligent & Robotic Systems*, vol. 78, pp. 359–375, 2015.
- [16] M. Ruderman, M. Iwasaki, and W.-H. Chen, "Motion-control techniques of today and tomorrow: a review and discussion of the challenges of controlled motion," *IEEE Industrial Electronics Magazine*, vol. 14, no. 1, pp. 41–55, 2020.
- [17] M. Spong, S. Hutchinson, and M. Vidyasagar, *Robot Modeling and Control*. John Wiley & Sons, 2005.
- [18] K. J. Åström and R. Murray, *Feedback systems: an introduction for scientists and engineers*. Princeton University Press, 2021.
- [19] M. Ruderman, *Analysis and compensation of kinetic friction in robotic and mechatronic control systems*. CRC Press, 2023.
- [20] C. P. Bechlioulis, Z. Douglgeri, and G. A. Rovithakis, "Guaranteeing prescribed performance and contact maintenance via an approximation free robot force/position controller," *Automatica*, vol. 48, no. 2, pp. 360–365, 2012.
- [21] A. De Luca, A. Albu-Schäffer, S. Haddadin, and G. Hirzinger, "Collision detection and safe reaction with the DLR-III lightweight manipulator arm," in *2006 IEEE/RSJ International Conference on Intelligent Robots and Systems*, 2006, pp. 1623–1630.
- [22] M. Ruderman, "Motion control with optimal nonlinear damping: from theory to experiment," *Control Engineering Practice*, vol. 127, p. 105310, 2022.
- [23] M. Ruderman, J. Reger, B. Calmbach, and L. Fridman, "Disturbance sensitivity analysis and experimental evaluation of continuous sliding mode control," *arXiv preprint arXiv:2208.06608*, 2022.
- [24] M. Ruderman, "On convergence analysis of feedback control with integral action and discontinuous relay perturbation," *Comm. in Nonlinear Science and Numerical Simulation*, vol. 145, p. 108698, 2025.